Fundamental Journals
International Journal of Fundamental Physical Sciences (IJFPS) ISSN:2231-8186
IJFPS, Vol 4, No 1, pp 13-25, March , 2014 *H. Shirinzadeh*
DOI:10.14331/ijfps.2014.330062
http://dx.doi.org/10.14331/ijfps.2014.330062

The Phenomenon of Colossal Magnetoresistance and Some Experimental Results

Haji Shirinzadeh

Department semiconductors Surface Physics and Thin films
Material and energy research Centre (MERC), Alvand Avenue, Tehran, Iran

Email: h_szadeh@merc.ac.ir

(*Received Dec 2013; Published March 2014*)

ABSTRACT

The Present $LaMnO_3$ material is anti ferromagnetic and insulting while replacing La with alkaline earth atoms changes take place in symmetry and crystal structure. Ferromagnetic interaction for example increase with do pant concentration χ and attains maximum at $\chi = 0.31$, beyond this level different type of antiferromagnetic interaction intra as well as inter-layer emerge which grown the overall magnetic behavior of the compound. We discuss semi covalent exchange interactions of four types. The nature of exchange viewed with the degree of overlap of the empty $Mn\ 3d$ level and the field O_{2p} level. Then most interesting case is $Mn^{3+} - O^2 - Mn^{4+}$ where exchange between Mn^{3+} and Mn^{4+} take place through hopping of holes at_{eg}levels from Mn^{4+} to Mn^{3+} viaO^{2-}. At each site the mobile hole spin is parallel to the localized case spin at t_{eg} and, thus, ferromagnetism is developed along $Mn^{3+} - O^{2-} - Mn^{4+}$ bonds. This double exchange is strong enough to suppress other exchange interactions. In this paper we are discuss the fundamental aspects of the double-exchange interaction, the impact of other important features like john-Teller effect, modulation of $Mn - O - M$ bond length and angle through A-site substitution ,charge carrier transport dependence on A-site radius, orbital ordering among the Mn^{4+} Mm^{3+} - Mn^{4+} network etc. the colossal magneto resistance (CMR) phenomena arises due to several cause. The paper reviews various observed aspects related to CMR to contribute to latest understanding of its physics. Some experimental results are given to illustrate some aspects.

Keywords: Thin films, CMR, Magneto Resistance

DOI:10.14331/ijfps.2014.330062

INTRODUCTION

The lanthanum manganite $LaMnO_3$ alkaline earth ions such as Ca, Sr etc show unusually large magneto resistance at low temperature. In order to distinguish it from multilayer's with magnetic-nonmagnetic or Ferro-antiferromagnetic, the former effect is named as colossal magneto resistance (CMR) and the later as Giant magneto resistance (GMR). The magnitudes are however many orders apart. The GMR arises due to spin orientation at interfaces while CMR has multiple origins dependent on doping concentrations. We will be concentrated with the physics of CMR, phenomenon. As usual, the discovery of the CMR effects took place in bulk materials, during study of doping effects, temperature dependence and magnetic field dependence. The similar properties can arise in granular material as well. For magnetic head read or record mode thin film configurations may be more acceptable for application aspect. Similarly attempt has been to find materials or conditions so that they need least possible magnetic field to display the significant effects. The attempts on application aspect are still in preliminary stage. But for a physicist the understanding of the intriguing mechanism possesses a still larger challenger. The present paper describes possible aspect related to CMR phenomenon, especially in manganite materials. It well known that simple electrical resistance arises

due to scattering of electrons with lattice, grain binderies, crystal defects, impurities etc. according to Mathiessen rule the contributions of lattice resistively (at low temperatures) and other contributions are additive, however all through we assume that materials are non magnetic. Here in magnetic materials such as transition metals from their own class due to presence of $3d$ and $4f$ electrons. The magnetic properties are displayed in *B-H* curves, domain formation, spin effects and magneto resistive properties. These aspects are well known. CMR phenomenon is related to doped or La-Deficient manganites. In order to restrict the length of the presentation here many issues are not included. We have directly discussed the mechanism. Some of our resent result on MBE grown epitaxial $LSMO$ films have been appended to provide an experimental flavor. The aim of this paper is to review the growth of colossal magneto resistance with in the early 1950s, perovskite $LaMnO_3$ compounds were synthesized and the unique relationship between the magnetic and electrical charge transport behavior was recognized (Jonker & Van Santen, 1950, 1953). To explain the relationship, a new indirect magnetic exchange interaction which considers the carrier transfer among the localized spin sites was invoked (Zener, 1951). The parent $LaMnO_3$ compound is anti ferromagnetic and insulating. The magnetic as well as crystallographic structure was studied by neutron diffraction technique by Wollan and Koehler for the entire family of $La_{1-x}A_xMnO_3$ ($x = 0.0 - 1.0$) compounds. Depending on the doping level x, the structure (both magnetic and crystallographic) and the symmetry undergo changes. Parent $LaMnO_3$ compound settles into a layered anti ferromagnetic and orthorhombic structure figure 1.with the increase in the doping level, ferromagnetic interaction starts increasing which attains maximum at $x = 0.31$. Beyond $x = 0.31$, the ferromagnetic interaction gives way to a different type of anti ferromagnetic interaction (which is intra as well as interlayer) which governs the overall magnetic behavior of the compounds till $x = 1.0$. The resistivity behavior within a certain characteristic temperature T_C or T_N changes from insulating to metallic at $x = 0.2$ and from metallic to insulating again at $x = 0.4$.

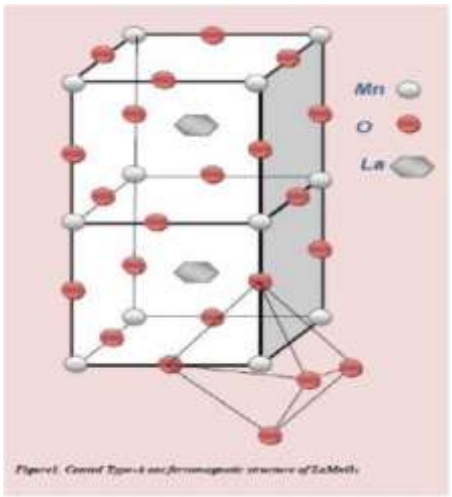

Figure.1 Canted type-A anti-ferromagnetic structure of $LaMnO_3$

The indirect exchange interaction mechanisms which dominate within a particular doping regime and the consequent electrical and magnetic behavior of the compounds are being discussed in the following paragraphs. The electronically active orbital in $LaMnO_3$ were found to be Mn_{3d}-O_{2p}. In the parent $LaMnO_3$ indirect exchange interaction takes place along $Mn^{3+} - O^{2+} - Mn^{3+}$ bonds.

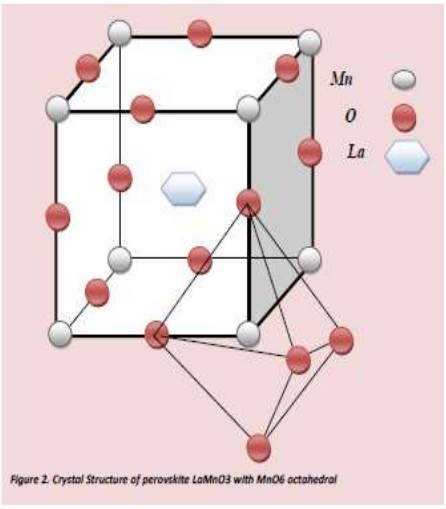

Figure.2 Crystal structure of perovskite $LaMnO_3$ with MnO_6 octahedral

In order to explain the observed magnetic interaction, (Goodenough, 1955) proposed a concept of semi covalent exchange where the degree of covalency (or the sharing time of valence electrons in full O_{2p} orbital with the ones in partially filled Mn $3d$ levels which depends on the spin - spin interaction between $3d$ and $2p$ valence electrons) changes and the prediction of the exchange differs from that of super exchange. There are four different cases of semi covalent exchange as identified by (Goodenough, 1955), Case I (Antiferromagnetic); Case II (Ferromagnetic); Case III (Ferromagnetic); Case IV (Paramagnetic) figure 2. The nature of the exchange varies with the degree of overlap of the empty Mn $3d$ level and the filled $O2p$ level. Case I considers the exchange along $Mn^{4+}-O^{2}-Mn^{3+}$and $Mn^{4+}-O^{2-}-Mn^{4+}$ Full oxygen $2p$ levels with two valence electrons interact and develop semi covalent bonding with Mn $3d$ levels. The electron with parallel spin to that of Mn d level spends more time on the Mn d level than that with anti parallel spin. Therefore, if both the electrons of O $2p$ level are involved with two Mn ions semi covalently, then an anti ferromagnetic interaction develops between $Mn^{3+}-Mn^{3+}$ and Mn^{4+}-Mn^{4+} The bonds are directed towards the O^{2-} ion and hence are shortest. Case-II, however, considers a lesser degree of overlap between the cation and the anions. Below a characteristic transition temperature, a mixed semi covalent and ionic bonding is developed where one $2p$ electron of oxygen is coupled ferromagnetic ally with one Mn ion while the other $2p$ electron is coupled ionically with another Mn ion. The ionic bonding leads to antiferromagnetic exchange coupling and hence the exchange among Mn^{3+}-Mn^{3+} in such cases is ferromagnetic. Case-III is dominated by the double exchange

among $Mn^{3+} - O^{2-} - Mn^{4+}$where the exchange between Mn^{3+} and Mn^{4+} takes place through hopping of holes at eg levels from Mn^{4+} to Mn^{3+} via O^{2-} At each site, the mobile hole spin is parallel to the localized core spin at t_{eg} and, thus, ferromagnetism is developed along Mn^{3+}- O^{2-}-Mn^{4+} bonds. This double exchange is strong enough to suppress other indirect exchange interactions. In the low doping regime, the double exchange interaction leads to canted type-A antiferromagnetism with a finite canting angle θ_0 between the localized spin at different $Mn - O$ layer. The hopping integral't' is related to the angle (θ) between the localized spin as $t = t_0\cos(\theta/2)$; t is maximum for $\theta = 0$ and zero for $\theta = \pi$ or antiferromagnetic coupling. Case-IV leads to paramagnetic interaction among Mn^{3+}, Mn^{4+}. The double-exchange interaction governed the ferromagnetism and metallicity below T_C. The ferromagnetic to paramagnetic and metal to insulator transition take place at T_C The charge transport and overall magnetic behavior of the entire family of materials are governed by the above mentioned fundamental exchange interactions. The structural symmetry also depends on the overall strength of the exchange interactions which, in turn, is governed primarily by the level of doping (or substitution at A-site) or $Mn^{3+}/\ Mn^{4+}$ ratio. The structure is determined by the internal energy of the system which is given by $H = [2J_{AFM}S^2 + 2J_{FM} + S^2 - tcos(\theta/2)N_Z$ (1). Where S is spin vectors; J is the exchange coupling, N is the number of magnetic ions and z is the number of charge carriers per unit cell. Minimization of the Gibbs free energy density $G = H - TS$ $[S = entropy]$ determines the structural symmetry under a doping level, x. Within the low doping regime, $x = 0 - 0.1$, the structure is mostly orthorhombic as most of the Mn ions are in Mn^{3+} states and the bonds Mn^{3+}-O^{2-}-Mn^{3+} are longer in one $Mn - O$ plane and shorter along the direction perpendicular to the plane. Within a $Mn - O$ mixed semi covalent and ionic exchange gives rise to weakly ferromagnetic interaction (case-II) while across two planes pure semi-covalent exchange leads to an antiferromagnetic interaction. This layered type anti-ferromagnetic structure was termed as type-A anti-ferromagnetism by (Wollan & Koehler, 1955). The bond lengths $(a1, a2, a3)$ are related as $a2 < a3 = a1$ with each $Mn - O$ plane having O^{2-} ions arranged around an Mn ion in the form of a rhombus rather than a square. The orthorhombic symmetry gives way to cubic symmetry at a transition temperature which is much higher than the Curie point. The covalent bond ordering sets in at that transition temperature whereas at Curie point the lattice parameters change following a second order transition. With the addition of Mn^{4+} ions, the Mn^{3+} ions are replaced randomly (within the low doping regime) and a covalent bond order develops within $Mn^{4+} - O^{2-} - Mn^{3+}$ bonds which leads to the shortening of the bond length. The $a2/a3$ ratio, therefore, tends to one and the double- exchange interaction lead to the development of metallicity. Of course, within a low doping regime, the type-A anti-ferromagnetism dominates. Increase in Mn^{4+} concentration leads to an increase in Curie point and decrease in resistivity. Within this low doping regime, therefore, a competition between the indirect semi-covalent exchange and the direct exchange develops which governs the nature of type-A anti-ferromagnetism. It has been shown by(De Gennes, 1960) that the spin structure is essentially canted with a finite canting angle θ_0 which depends on the carrier concentration x. This is the result of the fact that the internal energy of the magnetic lattice depends on the indirect exchange and double exchange energy. While the former varies with the angle θ between two localized spins in second order.

Schematic elect-spin configuration	Mn Mn seperation	Transition TEMPS	Resistivity	Case
AFM	Smallest	$T_c > T_t$	High	4
FM	Large	$T_c > T_t$	High	2
Paramagnetic	Largest	$T_t = 0$	High	3
Disordered Lattice				
Ferromagnetic	Small	$T_c > T_c$	Low	4

The Magnetic Coupling of Manganese ions in the Perovskite

Table 1. The magnetic coupling of the manganese ions in the $LaMnO_3$perovskite

The variation follows a first order relation in the later case. Hence the gain in energy through the double -exchange is higher than the loss through destabilization of the indirect exchange, and indeed, the canted structure is stable. Estimation of the canting angle θ_0 is discussed in a later section. With the increase in x, Mn^{4+} concentration increases which yields ferromagnetism within the entire lattice. Double exchange along Mn^{3+}-O^{2-} - Mn^{4+} and indirect exchanges along Mn^{3+}- O^{2-}- Mn^{3+} and Mn^{4+}- O^{2-}- Mn^{4+} govern the structural symmetry, magnetism and charge transfer behaviors. The double exchange leads to undistorted cubic lattice at a temperature even below Curie point. However, because of the elastic strain associated with Mn^{3+}-O^{2-}-Mn^{3+} bonds, the structure can settle into a rhombohedra symmetry over a doping range $x = 0.1 - 0.25$x. For $x > 0.25$, cubic symmetry is most likely. The resistivity reaches a minimum for $x = 0.31$ (Goodenough, 1955) which can be shown by imposing the condition that within a disordered lattice the optimum magnetization occurs when largest number of Mn^{3+} ions are coupled with one Mn^{4+} ion. The minimum resistivity, of course, is higher than Mott maximum resistivity (N. F. Mott & Davis, 1979) p_{max} for a disordered lattice undergoing metal-insulator transition. Therefore, the nature of metallicity within the metallic $LaMnO_3$ system is still a contentious issue. With further increase in x close to 0.5, the number of $Mn^{3+} and\ Mn^{4+}$ ions becomes equal which leads to a new ordering among the ions. The covalent bond order is set at a transition temperature which is different from Curie point. The ordering among $Mn^{4+} - Mn^{3+}$ and consequent charge ordered state yield a new magnetic ordering called CE-type. The ordering in $Mn^{3+} - Mn^{4+}$ may take place along alternate $(110), (111) or\ (100)$ planes. However, the (110) plane

arrangement is most likely as it leads to minimum elastic energy and lattice strain $(a3-a2)/a3$. The charge ordered state leads to insulator behaviour below a transition temperature T_{Co} as a result of strong-correlation across the ordered $Mn^{3+}-Mn^{4+}-Mn^{3+}-Mn^{4+}$ planes. Beyond $x=0.5$, the concentration of Mn^{4+} becomes higher which gives rise to strong G-type anti-ferromagnetic interaction along the $Mn^{4+}-O^{2-}-Mn^{4+}$ bonds. The composition exhibits anti-ferromagnetic insulating behaviour below T_N. The structural symmetry changes from tetragonal to cubic as x approaches 1 from 0.5.The structure, electrical and magnetic properties of the entire family of $LaMnO_3$L materials, therefore, appear to be governed by the complex exchange interactions like semi-covalent exchange, ionic exchange and double exchange. Double exchange, incidentally, involves movement of the electrons or holes from site to site in order to develop an interaction between two localized magnetic ions. Such an exchange interaction leads to ferromagnetism since the travelling electron ($hole$) must have its spin parallel to the core spin (S=3/2) at any localized site. This is the consequence of strong Hund's coupling J between the core spin at eg level and the mobile electron at eg level. Electron with anti parallel spin to the core spin cannot travel to a respective localized site. Therefore, by modulating the spin vectors at any localized site one can modulate the carrier transport. The transport also depends crucially on the $Mn-O-Mn$ bond length and angle and the effect of orbital ordering among $Mn^{3+}-Mn^{4+}$ network. In the following paragraphs, we shall discuss the fundamental aspects of the double-exchange interaction; the impact of other important features like Jahn-Teller effect, modulation of $Mn-O-Mn$ bond length and angle through A-site substitution, dependence of charge carrier transport on average A-site radius and A-site mismatch or variance (σ^2); orbital ordering among the $Mn^{4+}-Mn^{3+}-Mn^{4+}$ network etc. We shall also try to develop a coherent picture of the manganite physics in order to lay bare the key factors which should be looked into for improving the magneto-resistivity. For any device application of these materials, along with the intrinsic magneto-resistivity extrinsic magnetoresistivity also assumes importance.

DOUBLE-EXCHANG INTERACTION

(a) Energetic of charge transfer process

The correlation between the electrical charge transport and magnetic properties as a function of applied magnetic field in the case of manganites could be explained by invoking a new kind of indirect exchange mechanism(Zener, 1951). An additional degree of freedom is involved in this kind of exchange mechanism: movement of electrons (holes) from one magnetic ion to another through a non-magnetic atom which, in turn, leads to the development of an exchange interaction between two magnetic ions. It seems to be another variant of the RKKY interaction where interaction between two localized spins takes place through mobile electrons. Of course, RKKY is a long range interaction while double exchange is restricted within a short range. The travelling electron ($hole$) carriers its spin parallel to the core spin vectors of the magnetic ions. The exchange coupling J^* thus developed is, of course, very small compared to the Hunds coupling J between the core and outer spins. J^* is defined by the Hamiltonian H which considers the transport of electrons from one site to another multiplied by the wave functions ψ_1 and ψ_2 which are linear combinations of the degenerate localized electron states. The coupling energy J^* is related to the diffusion coefficient D of the Mn^{4+} ions (since the charge carrier transport along $Mn^{3+}-O-Mn^{4+}$ is equivalent to the diffusion of Mn^{4+}ions) by the relation $D=a^2J^*/h$, where a is the lattice parameter, h is the Planck's constant. The diffusion coefficient D, in turn, is related to the conductivity $\sigma=\frac{n^2eD}{K_BT}$ where n is the number of Mn^{4+} ions per unit volume. Therefore, the conductivity can be related to the exchange energy J^* Thus, the observed charge transport behaviors of the manganites could be quantitatively calculated following this double-exchange mechanism. Detailed calculation of the energetic of the double-exchange mechanism was performed by Anderson and Hasegawa (Anderson & Hasegawa, 1955).One consequence of their calculation is the direct relation between the carrier hopping matrix element $'t'$ and the angle $'\theta'$ between the localized spin vectors $'S_{ij}$ at $i-th$ and $J-th$ sites. In its simplest form the calculation considers transfer of an electron from a partially filled d orbital of a magnetic ion to another similar magnetic ion via full p-orbital of an oxygen atom. In manganites, such transfer takes place over $Mn^{3+}-O^{2-}-Mn^{4+}$ bond. Because of octahedral MnO_6 field, the d-levels are split in eg and t_{2g} levels with d_z^2 and $d_x^2-_y^2$ forming the eg level and d_{xy},d_{zx},d_{yz} forming the t_{eg} level. Strong intra-atomic Hund's coupling J between eg & t_{2g} leads to parallel (i.e. ferromagnetic) alignment of the spins. The energetic of the transfer of an electron ($or\ hole$) over $Mn-O-Mn$ bond is calculated by considering three orbitals and three configurations: mobile electrons $d_1(Mn^{3+}),d_2(Mn^{4+})$; closed p-shell at system p; core d electron $d_1^{'}(Mn^{3+}),d_2^{'}(Mn^{4+})$; configurations.

I: $Mn^{3=}-O^{2-}-Mn^{4+}\ [d_1^{'}-d_1-p^2-d_2]$
II: $Mn^{4+}-O^{2-}-Mn^{3+}\ [d_1^{'}-p^2-d_2{'}d_2]$
III: $Mn^{3+}O^{1-}-Mn^{3+}\ [d_1^{'\,d_1}-p-d_2d_2^{'}]$

The electron transfer process then becomes the interaction of the configurations. For any one of the configurations I and II, the process well end on either II or I via configuration III. By considering two spin states α,β at Mn_I site and $\alpha'\beta'$ at Mn_{II} site, and $\alpha'\beta'$ at Mn_{II} site, and noting the inter-atomic coupling energy as J^* while the transfer matrix element between $Mn_I\ and\ Mn_{II}$ as b, one can calculate the energetic of the charge transfer process. The transformation relations between α,β and $\alpha'\beta'$ are

$$\alpha=\cos\left(\frac{\theta}{2}\right)\alpha^{'}+\left(\frac{\theta}{2}\right)\beta^{'} \quad (1)$$

$$\beta=-\sin\left(\frac{\theta}{2}\right)\alpha+\cos\left(\frac{\theta}{2}\right)\beta^{'} \quad (2)$$

Using the transformation energy matrix, it is possible to show that

$$E=\frac{1}{2}J\ \pm[J^2\left(S+\frac{1}{2}\right)^2+b^2\pm 2Jb\left(S+\frac{1}{2}\right)cos\left(\frac{\theta}{2}\right)]^2 \quad (3)$$

Which for the limiting case $J>>b$ J>> b take the form

$$E \cong -JS \pm bcos\left(\frac{\theta}{2}\right) \quad (4)$$

The $\pm$ sign signifies the transfers for high spin and low spin arrangements at Mn_I and Mn_{II}.Obviously, the transfer energy $t \approx bcos\left(\frac{\theta}{2}\right)$. Where cos $(\frac{\theta}{2})$ is given by $(S_1 + S_2)/2S$ [S_1 and S_2 are spin vectors at Mn_I and Mn_{II} respectively]. The overall exchange energy thus varies linearly with $S-$ clearly at variance with the Heisenberg type exchange energy expressions of any other direct or indirect exchange where $E \sim S^2$. Moreover, the energy of the double exchange interaction is symmetric with respect to the average energy for high spin and low spin arrangement. Hence the average energy $< E >$ becomes independent of $S_1 + S_2$ and since the susceptibility χ of the system depends on$< E >$, χ also, in turn, becomes independent of $S_1 + S_2$. The temperature dependence of χ is found not to follow Curie-Weiss law in that case. Surprisingly, manganites, for which this double-exchange interaction is expected to be valid, do follow Curie-Weiss law. This is probably an indication that the double-exchange mechanism is not sufficient to explain the correlation between electrical charge transport and magnetization in manganites. We shall return to this point later. There are several consequences of the double-exchange interaction: for example, the ferromagnetism-driven metallic resistivity pattern, metal-insulator transition at a particular Mn^{4+}concentration $(x = 0.2)$ within the parent insulating $LaMnO_3$lattice, subtle change in spin arrangement and hence magnetism within the sub lattices depending on the relative strength of the super exchange and double exchange interactions as a function of x etc.

(b) Canted Type-A Anti Ferromagnetism In $La_{1-x}A_xMnO_3$

One direct consequence of strong double-exchange interaction is a distorted spin structure in $LaMnO_3$ with low carrier concentration. This was shown theoretically by (De Gennes, 1960) and experimentally by several groups (Chakraborty, Bhattacharya, & Maiti, 1997; Kawano, Kajimoto, Kubota, & Yoshizawa, 1996). Such distortion results from linear dependence of the double energy on the spin vectors S of the magnetic ions vis-à-vis Quadratic dependence of other indirect exchange energies on the spin vectors. It leads to stabilization of the lattice through finite carrier hopping over the canted spin structure. For a layered anti-ferromagnetic arrangement, which represents the spin structure in $LaMnO_3$ within low carrier concentration, the canting angle θ_0 at a low temperature can be evaluated as a function X by minimizing the total exchange energy $= E_d + E_{ex}$. The double exchange energy E_d is given by

$$E_d = N_X\left[-\zeta_0 b' - \zeta_0 \cos\left(\frac{\theta}{2}\right)\right] \quad (5)$$

While the order indirect exchange energies are given by

$$E_{ex} = N_Z J' S^2 + N_Z |J| S^2 cos\theta_0 \quad (6)$$

Minimizing E with respect to θ_0 we find

$$\cos\left(\frac{\theta_0}{2}\right) = \frac{bx}{4JS^2} \quad (7)$$

and

$$-E = N[-z'\mathrm{J'S^2} - \chi \mathrm{z'b'} - \frac{\frac{z}{J}}{S^2} - \frac{\frac{\left(\frac{z}{8}\right)b^2\chi^2}{1J}}{S^2} \quad (8)$$

for a finite b and x, therefore, θ_0 is finite which points out a canted anti-ferromagnetic structure in $LaMnO_3$. Such arrangement leads to a spontaneous non -zero magnetization within the sub-lattices and hence the response of the system under an applied magnetic field is found to be sharp(Chakraborty et al., 1997).

Extension of the canted spin structure model at higher temperature is possible by using either spin wave treatment or molecular field treatment. Above a finite critical temperature T_1, the spin arrangement changes into Ferro or anti-ferromagnetic arrangement. The stable structure can be obtained by minimizing the Gibbs free energy $G = H - TS$ where H is the internal energy and S the entropy. In order to calculate the equilibrium state for the vibrating and interacting ions, a statistical distribution of the molecular field is considered $\omega_n(s) = \left(\frac{1}{v}\right)\exp(\lambda_n.\frac{S}{S})$ (While the average double exchange energy is $E_m = -\zeta_0 b <\cos(\frac{\theta}{2})> -\zeta_0{}'b' <\cos(\frac{\theta'}{2})>$ Expressing the thermal averages $<\cos(\frac{\theta}{2})>$ and $<\frac{cos}{\theta'}/2)>$ in terms of Legendre polynomials $P(cos\theta)$ and considering the distribution of the molecular fields for ω_1, ω_2 etc, one can derive the expressions for $H(= E_{ex} + E_D)$ and

$$TS: -Ts = Nk_B\, T\int_{-1}^{+1}\omega(x) In\,\omega(x)dx$$
$$= NK_BT(\lambda m - 1nv)$$

where

$$m = \frac{1}{v}\int_{-1}^{=1} du.u.e^{-\lambda u} \quad (9)$$

is the average saturation of the magnetization in any Sub lattice $= conth\lambda$ (Langevin function)

$$E_D = \frac{2N_{XZ}}{j_0^2(-i\lambda)} - \sum_{i=0}^{\infty}\frac{ji^2\,(-i\lambda)}{(2l-1)(2l+3)}\, x[\xi_0 bP_i\cos(\theta) + \xi_0' b' \quad (10)$$

$$E_{ex} = -Nm^2(Z'J' + zJ\,cos\theta) \quad (11)$$

Minimization of $E_D + E_{ex} - TS$ with respect to θ or λ gives the canting angle θ_0 as well as the critical temperature beyond which the spin arrangement changes from canted structure to Ferro or anti ferromagnetic structure. Setting $v = cos\theta$, one can show that for large λ (i.e., low temperature) the canted arrangement is stabilized where V_m lies within $-1 < V_m < 1$. For largeλ, $V_m > -1$ (the equilibrium arrangement is ferromagnetic) or V_m <-1v (the equilibrium arrangement is anti-ferromagnetic).

(c) Metal - Insulator Transition

The role of double exchange interaction can be observed in driving the insulator state into a metallic state. Apart from two distinct class of materials: insulators and metals where in the former class the valence band is fully filled with the Fermi

level E_f in the band gap and in the later class the band is partially filled with the Fermi level E_f within the band, there are other classes of materials as well where the insulator state is either correlation driven or disorder (randomness) driven or driven by both of them. The transition metal oxides, normally, fall into this category. The insulator to metal transition in such cases can be engineered by changing the parameters like charge carrier concentration, bond angle and length, temperature, substitution level etc by which the Fermi level EF can be made to pass from the band gap region to the filled band region. In other words, the parameter $(E_C - E_F)$ becomes negative from positive (E_C=conduction band).which signifies an insulator to metal transition.

The concept of correlation among the electrons (i.e., repulsion between electrons at the same site) and the development of insulating state as a result of that have been provided by Mott (Lee & Ramakrishnan, 1985) and this class of insulators is called Mott insulators. Randomness in the atomic potential v as a result of either distribution of atoms with varying v within the lattice or distribution of the atom - atom distance (i.e., periodicity) or both can lead to the development of insulating state where the electron wave remains localized or confined within a small radius centering on an atom. Such disorder-driven insulator state is normally known as Anderson localization (Goodenough, 1955). In reality, of course, both the electron correlation effect as well as the disorder effect are present which govern the localization - delocalization of the charge carriers or insulator-metal transition. The band structure develops a gap Δ which drops precipitously to zero at the critical condition of insulator to metal transition. The basic factor involved in the metal-insulator transition is the interplay between electron kinetic and potential energies.

While the electron kinetic energy is governed by the momenta and the degree of orbital overlap etc which determine the Fermi level, the band width etc, and the potential energy is governed by various correlation effects like electron-electron correlation, electron-phonon correlation, spin-spin correlation etc.

The transition from metal to insulator state or vice versa is governed by the values of the ratio of suitable parameters of the kinetic and potential energies like $\frac{t_{eff}}{\lambda_{eff}}, \frac{t_{eff}}{J_H}, t_{eff}/V$ etc where t is the transfer hopping matrix element and, λ_{eff} J_H are the electron-phonon coupling parameter, magnetic exchange coupling energy, atomic potential etc. The transition as a function of critical parameters like the carrier density x, average bond length or temperature or even the frequency of irradiating electromagnetic pulse etc can be a smooth cross-over (second order transition) or a sharp jump at a specific value (first order transition).

In the case of the transition metal oxides, the insulator state is characterized by a band gap Δ (with the Fermi level E_F lying at the gap) which is often created by the magnetic correlation effect (periodic spin-spin correlation effect of the local spins or the coupling between the spin of mobile electrons and localized ions, i.e., magnetic polar on formation). The band gap Δ is either Mott-Hubbard gap (developed as a result of correlation among $'d'$ level electrons and splitting in the energy levels) or the charge - transfer gap (where the gap is created between the d and p levels as a result of higher degree of overlapping among them).

Accordingly, the materials are categorized as Mott-Hubbard insulator or charge-transfer insulator. The parent $LaMnO_3$ compound is A-type anti-ferromagnetic and insulator. The electronically active band is Mn^{3+}-O^{2-}-Mn^{3+} where the mn d levels are split into e_g (higher) and t_{eg} (lower) levels (comprising of $d_Z^2, d_Z^2{-}_y^2$ and d_{xy}, d_{zx}, d_{yz} levels respectively) as a result of crystal field of MnO_6 octahedral within the $LaMnO_3$ cubic perovskite structure. The d^4 state of Mn^{3+} represents the high spin state ($S = 2$) due to strong Hund's coupling between t_{2g} and e_g electrons which gives rise to ferromagnetic alignment among them. Active eg level, however, undergoes further splitting into separate d_z^2 and $d_x^2{-}_y^2$ levels as a result of asymmetric filling and consequent distortion with closer overlap among $d_x^2{-}_y^2 - p$ orbital and lesser overlap among $d_z^2 - p$ orbitals. This effect is known as Jahn-Teller effect(Imada, Fujimori, & Tokura, 1998).

The splitting gives rise to a band gap Δ and since the Fermi level E_F lies in the band gap, the parent compound is an insulator. Substitution of La^{3+} site by divalent Sr, Ca, Ba, or Pb gives rise to hole doping at Mn^{3+}. Strong double exchange along ferromagnetic $Mn^{3+} - O^{2-} - Mn^{4+}$ bonds yields coherent carrier hopping and metallization. The band gap Δ drops to zero at a carrier concentration $x \approx 0.2$ and the ground state becomes metallic at such a doping level. This double-exchange driven metallicity is the key feature of these compounds which yields large magneto resistivity. The ferromagnetic metallic state can be considered as evolved from the basic Hamiltonian

$$H = -\frac{\sum t_{ij} d_i^+ d_j + J_H \sum S_c^i d_i^+ \sigma d_i + h S_c}{S_c} + H_{\Gamma\Gamma} \qquad (12)$$

through suitable variation of the parameters like t, J_H, electron-phonon coupling constant etc. The metallic state, of course, bears signature of Non-Fermi liquid (Imada et al., 1998). Yet it has clear correlation with the ferromagnetism and the electron bandwidth W is directly proportional to the ferromagnetic Curie point T_c The generic resistivity (ρ) vs. temperature (T) behavior of this class of materials over a doping range $x = 0.2 - 0.4$, is metallic below T_C and insulating above it (Fig.4). Therefore, even the metallic compound undergoes a metal-insulator transition at T_C. One of the reasons behind $M - I$ transition could be breaking of ferromagnetic order above T_C. The paramagnetic state leads to strong scattering and consequent localization of the charge carriers. However, T_C, can be improved by applied magnetic field which suppresses the scattering and enhances the metallization and thus gives rise to colossal magnetoresistivity.

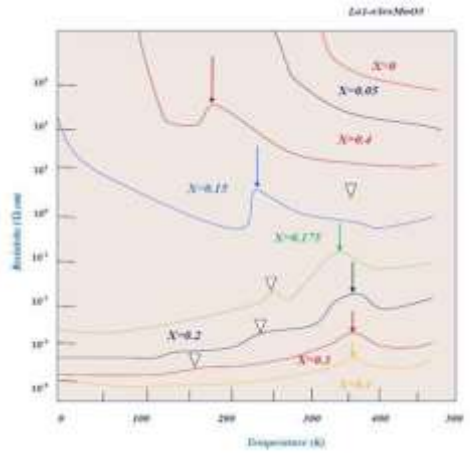

Figure.3 Figure 3 Resistance vs T for $La_{1-x}Sr_xMnO_3$ for various x values the transition as determined by magnetization measurements

JAHN-TELLER EFFECT

The Jahn-Teller effect (Imada et al., 1998), in the molecules is the non-degeneracy in the d-levels as a result of asymmetric filling and overlapping of d level bands with the legends. The splitting of the band is associated with lattice distortion as the degree of overlap of the valence electron wave functions at d-levels differ at different directions and hence lead to an asymmetric bond length distribution. In the perovskite $LaMnO_3$ compound, Mn^{3+} ions are Jahn-Teller active because of asymmetric overlap of $Mn\ eg$ levels with the $O\ 2p$ levels. The $Mn^{3+}-O^{2-}$ bonds along $x-y$ directions are shorter (signifying strong overlap) while that along z-axis is longer (depicting weaker overlap). The splitting at $Mn^{3+}\ eg$ level yields lattice distortion which makes the crystallographic structure as disordered, i.e., one having lower symmetry than the cubic. The distorted structure localizes the charge carriers and hence the electron kinetic energy drops. The binding energy $E_{\Gamma T}$ (or the coupling energy with which the lattice distortion is coupled to the charge carriers to form the polarons) with respect to the electron itinerancy double exchange energy E_d governs the switching from polaronic conduction (thermally activated polaron hopping) above T_C to Fermi-liquid like metallic behaviour below T_C. The importance of Jahn-Teller effect in governing the charge-transport and magnetization behavior in $LaMnO_3$was pointed out by(Millis, Littlewood, & Shraiman, 1995). They solved the double-exchange model and calculated the electron kinetic energy which, in turn, can be related to the T_C. T_C, thus found, and turn out to be an order of magnitude higher than the experimental value. The resistivity and the magneto resistivity too, appear to have such discrepancy. In order to reconcile the difference, they pointed out that the JT active Mn^{3+} ions lead to the localization of the charge carriers through strong electron phonon coupling and, therefore, only a coupled model of double-exchange interaction and JT effect can reproduce the experimentally observed behaviors with reasonable accuracy. The Hamiltonian describing this model is, $H = H_{el} + H_{\mathrm{JT}}$.

$$H = \sum_{tij} d_i^{\dagger} d_j + J_H \sum S_e^i , d_i^{\dagger} \sigma d_i + \frac{hS_c}{S_c} + g \sum d_j^{\dagger} Q^{ab}(i) d_j + (\frac{k}{2}) \sum Q_2(j) \quad (13)$$

where $d^{\dagger}$ is the creation operator at the outer-shall d level, g is the electron-phonon coupling constant, k is the phonon stiffness factor, J_H is the Hund's coupling. Solution of this Hamiltonian for different values of electron-phonon coupling constant yields the T_C and the resistivity observed in this class of materials. Because of Jahn-Teller effect, the mean displacement of the oxygen atoms in the $Mn-O-Mn$ bonds changes and from the measurement of such shift one can estimate the coupling energy. After this initial proposal regarding the relevance of Jahn-Teller physics in the manganites, many experiments have been carried out to show the role of Jahn-Teller effect in governing the properties of the manganites : optical(Jin et al., 1994), thermal(Hwang, Cheong, Radaelli, Marezio, & Batlogg, 1995), isotope effect(Van Slyke, Chen, & Tang, 1996) to name a few

CHARGE-ORDERING EFFECT

The properties the manganites are governed by a complex interplay of charge -spin and lattice degrees of freedom as any interaction like charge-charge or spin-spin or charge-lattice etc. is modulated by another degree of freedom. Or, in other words, by changing any one of them, the interaction between the other two can be changed. The ordering of the charges across the lattice gives rise to the charge-order insulating state as a result of strong electron-electron correlation effect. For the composition $la_{0.5}Ca_{0.5}MnO_3$, equal number of $Mn^{3+}$and Mn^{4+} ions settle into such an ordered state. The periodicity of this order may or may not be commensurate with the underlying lattice order. However, since charge ordering further reduces the electron kinetic energy and hence narrows down the eg level electron bandwidth, an insulating state develops below a characteristic temperatureT_{CO}. The development of charge-ordered insulating state, once again, can be tuned by average A-site radius $< \Gamma_A >$ (Rao & Cheetham, 1997) or the effective $Mn-O-Mn$ bond length and angle. For example, in $La_{0.55}Sr_{0.5}MnO_3$, $< \Gamma_A > \approx$ 1.26Å and no charge ordering takes place, whereas in $Nd_{0.5}Sr_{0.5}MnO_3$ $< \Gamma_A > \approx$ 1.24Å or $Nd_{0.5}Ca_{0.5}MnO_3$ $< \Gamma_A > \approx$1.17 Å and the charge ordering takes place below 150 and 250K respectively. Therefore, it appears that for$< \Gamma A > \leq 1.17$, charge-ordered state appears below T_{Co} whereas if $< \Gamma A >$ lies between $1.17 - 1.24$Å both charge ordered as well as ferromagnetic transition occurs below T_{CO} and T_C with T_C For $< \Gamma A > \geq 1.24$Å, charge ordered state does not develop. The charge-ordered insulator state can undergo a first order transition into a metallic ferromagnetic state under a high magnetic field ($> .5T$) (Majumdar & Littlewood, 1998). Such melting of the charge -ordered state under a switching field can also be utilized in many applications. The charge-ordered state can sometimes settle into a new pattern which is known as stripes (Hwang, Cheong, Ong, & Batlogg, 1996). Instead of uniform $Mn^{3+}-Mn^{4+}-Mn^{3+}-Mn^{4+}$ etc network pattern across the entire geometrical space, stripes of one species

sandwiching stripes of other species can also develop at any commensurate charge carrier density or band filling factor x. The reason behind such order is the minimum energy consideration of the electron charge density and lattice interaction. Along the stripe the electron charge density maintains a periodicity which is commensurate with the lattice whereas across the stripe the periodicity is different from that of the underlying lattice. This arrangement certainly is different from the chequerboard type arrangement. In $La_{0.5}Ca_{0.5}MnO_3$, it has been observed that stripes of $Mn^{3+}\ O_6$ (Jahn-Teller stripes) along with the stripes of $Mn^{4+}O_6$ are formed (Li, Gupta, Xiao, & Gong, 1997) with two JTS sandwiching one $Mn^{4+}O_6$ stripe. This block two $Mn^{3+}O_6$ stripes with one $+MN^{4+}O_6$ stripe in between appears to be the basic building block of the entire arrangement. The lattice parameter of this stripe phase structure is $3_{a0}\ if\ x = 1/2$ whereas it is $4_{a0}\ if\ x = 3/4$ and $5_{a0}\ for\ x = 4/5$ where a_0 is the lattice parameter of the basic cubic lattice. While such stripe phases (with quantum fluctuation) form at commensurate band filling x (Venkatesan, Rajeswari, Dong, Ogale, & Ramesh, 1998) in high T_C superconductors as well, in perovskite manganites the stripe phase are having a static order. With the discovery of the stripe phases in manganites, the stripe physics assumes special importance as it underscores the importance of the correlation effects as opposed to hybridization effect of the electronic charge density distribution.

OTHER.ISSUES IN THE PHYSICSOF THE MANGANITES

The double exchange energy together with the JT energy appear to be not quite sufficient in describing the electrical, thermal, optical, magnetic and a whole lot of related physical properties. It has already been pointed out that the physics of the perovskite manganites is dominated by the interplay of charge, spin and lattice degrees of freedom. Therefore, correlation effects have a major role to play in controlling the one electron bandwidth W and it is varies as $W\alpha\ W_0 \exp(-U/h\omega)$. Here W_0 is the bare electron bandwidth and U is the correlational binding energy. Recently, many new observations have been made regarding the correlation effects and their influences even below T_C. For instance, measurement of optical conductivity$\sigma(\omega)$ suggests that the coherent Drude part (which is the contribution of the double-exchange interaction) is roughly two orders of magnitude smaller than the incoherent background scattering below T_C (Okimoto, Katsufuji, Ishikawa, Arima, & Tokura, 1997). Such observation points out that the correlation effects are dominant at lower temperature also. Therefore, the simple picture that below T_C the properties are governed by double-exchange while above T_C polaronic activated hopping conduction (as a result of JT effect) dominates breaks down. Moreover, this class of materials has been identified as charge-transfer insulators with $hole$ doping at O^{2-} (Ju, Sohn, & Krishnan, 1997). The conduction, of course, takes place through ferromagnetic exchange and hence in the metallic regime the resistivity does scale with $(M/M_{s)}$. Recently, it has been proposed that the metal-insulator transition around T_c is governed by the formation and collapse of the bipolarons (Alexandrov & Bratkovsky, 1999). Below T_C, the bipolaron coupling breaks down due to ferromagnetism while above T_c, strong coupling of the bipolarons yields very high resistivity and activated hopping behaviour. The bipolarons form around O^{2-} sites and develop a static order whereas the bipolarons in $high - T_C$ superconductors appear to be more mobile. Of course, at a very high temperature above T_C, the mobility of the bipolarons can be higher than what is observed near T_C. The physics and the mechanism of the bipolaron formation and dynamics are yet to be settled. It appears, therefore, that this intriguing problem will keep the condensed matter researchers captivated in foreseeable future.

EXPRIMENTAL

The crystal growth was carried out by Molecular Beam Epitaxy system. Equipped with two independent electro beam evaporation and four effusion cell (K-shell) the pressure of the MBE chamber is $4x10^{-10}$torr. During deposition growth pressure were controlled at below $3x10^{-9}$torr. Deposition $rate{\sim}0.1\ A/S$ the film thickness and deposition rate were measured by the quartz crystal thickness monitor (Lebold inficon XTC & IC 6000) and calibrated by ellipsometry and $X - ray$ reflectivity analyses. To able the growth of high quality samples we have done organic chemical cleaning through ultrasonic above $1/2$ then ultra high vacuums in the MBE system. They were then out gassed at $800 - 900^0C$ an hours. In further cleaning $10 - 15$ monolayer's oxygen contamination cleaning with an ion beam, the deposition results in enhanced adhesion and reduced oxygen contamination. It effect on lattice distortion. Pure elements (99.99%) of La, Mn, Sr were used. The substrate temperature was varied two types $500 - 300^oC$ to reduce the inter diffusion at the interfaces as Non eqalibarom deposition .we exam crystal structure of the film surface were in-situ and throughout all the growth $600 - 650$ electron Volt for the foundation $Si(111)7x7$ wafer, through reflection high energy electron diffraction (RHEED).

(a)

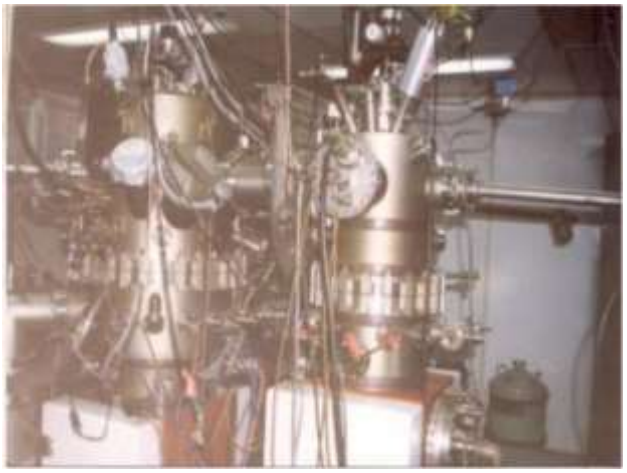

(b)

Figure.4 Photograph of preparation Chamber (a) and MBE deposition system (b) (S.PAlein#SII/745 Picotorr 450)

SAMPLE PREPARATION

All the thin film samples used in present study were prepared in an oil free Varian MBE-360 S.P.A.Lein # SII/745 PICOTORR 450 thin film deposition system .The preparation chamber 14" in diameter is of stainless steel (Fig 2.(a,b)which meander type water cooling arrangement. Rough pumping of the chamber is done by turbo pump $V450$ units and final base pressure of $10^{-11}\ torr$ is obtained by $120 l/s$ Star cell VacIon pump. The chamber has a Ferro fluid rotating feed through to accommodate a planetary substrate holder of stainless steel in which 4" die can be loaded at one time different geometrical dimension of wafers. There are two electron guns of $10KW$ each with a water cooled hearth of single $40cc$ crucible and anther four $30\ cc$ crucibles. The thinness of the film is measured in - situ by three quartz crystal thickness monitor at different angle as coals fitted with an $Infio\ XTC$ process controller. The pressure in the chamber is measured by multiple pump control unit 929 Varian ionization gauge of Bayard-Alperd Type.

ELECTRICAL CHARGE AND ELECTRONIC TRANPORT PROPERTIES

Electrical charge its dynamics and interplay of magnetic exchange interaction on transport properties of disordered perovskite-type oxides and Colossal magnetoresistance (CMR) material found in systems such as $LaMnO_3$ and its substituted derivatives , have been the subject of interest for decades. This interest has been renewed because of their possible use as electrodes in high - temperature solid oxide fuel cells(Chakraborty et al., 1997; Goodenough, 1955; Honda, Fujimoto, & Nawate, 1996; Imada et al., 1998; N. Mott, 1961). However most of the studies were concentrated within a small range of substituent or within a limited range of temperature either in the low- or in the high-temperature range the salient features of this subject as available in the literature has been briefly reviewed here. Pure $LaMnO_3$ is a p-type semiconductor (Celotta, Pierce, & Unguris, 1995; Speriosu et al., 1993). The intrinsic $p-type$p conductivity arises due to the formation of cation vacancies and consequently, due to the $hole$ motion in d-electron energy levels of manganese ions (Bass & Pratt Jr, 1999). Thus, the electrical conductivity of the material can be enhanced merely by substituting a lower-valence ion on either at the $La\ Site\ (A\ site)$ or $Mn\ site\ (B\ site)$. Doping of $LamNO_3$ with various lower-valence cation such as strontium , calcium, barium , nickel , magnesium , lead, sodium , potassium and rubidium has been found to have enhanced the electronic conductivity of the material due to increase in MnO^{4+} content as a result of substitution of La^{3+} by these divalent or monovalent ions (Baibich et al., 1988; Bloemen, Van de Vorst, Johnson, Coehoorn, & De Jonge, 1994; N. F. Mott & Davis, 1979; Palstra et al., 1997). Among all substituent ions, most of the studies have been carried out by doping alkaline-earth metals, particularly with strontium substituted at lanthanum site $La^{3+}+Sr^{3+}$.

$$LaMnO_3 \xrightarrow{SrO} La^{3+}_{1-X}\ Sr^{2+}_x Mn^{3+}_{1-x}\ Mn^{4+}_x O_3, \qquad (14)$$

The pure strontium (alkaline-earth) substituted $LaMnO_3$ exhibit thermally activated conductivity with the substituted material passing a smaller activativation energy (Honda et al., 1996; Imada et al., 1998; N. F. Mott & Davis, 1979). The conductivity of pure and substituted lanthanum manganite above 400K has been described by a small polaron hopping conduction model (Chakraborty et al., 1997; Honda et al., 1996; N. F. Mott & Davis, 1979). The basic step is an electron $(hole)$ transfer between two Mn ions via the bridging oxygen ion i.e., through the network $Mn^{3+}-O^{2-}-Mn^{4+}$.Magnetic properties of Pure $LaMnO_3$and that substituted with Sr. The variation of magnetisation with temperature has been studied for un substituted lanthanum manganite $(LaMnO_{3-\delta})$ at different temperatures $(800-950^0C)$ in vacuum inUHV system, and for the series $La_{1-x}Sr_xMnO_3$ $(0 \le X \le 0.50)$at 950^0C different applied magnetic field from $(100_{Oe}\ to\ 10K_{Oe})$ in the temperature range $20-300K$. According to their magnetic properties, these compositions may be classified into three major groups. The compositions in the first group consist of Mn^{3+} as the major magnetic ions. The amount of Mn^{4+} the other type of magnetic ion is comparatively less in these samples. And compositions with $0.17 \le X \le 0.50$ in. $La_{1-x}Sr_xMnO_3$. Series, and then consists of compositions with have Mn^{4+} as the major magnetic ions. The compositions with $X > 0.50$ in the series $La_{1-x}Sr_xMnO_3$ constitute this group the magnetic behavior for the second sample is shows in three representatives (Figure.3). We have plotted σ_m versus temperature curves for $La_{0.70}Sr_{30}MnO_3$ and $La_{0.}Sr_{0.50}MnO_3$ sample. The antiferromagnetic character is very weak for these samples. This is evident from the result that the net magnetic moment at $20k$ for these samples is much higher than that for pure $laMnO_3$ annealed at 900^0C. At $100\ O_e$ A week antiferromagnetic behavior is still present particularly at low temperatures. Higher magnetic fields reduce the antiferromagnetic behaviour further as seen from SEM photographs of $LSMO$ in Figure.6(a.b.c.d), the annealing temperature as well as duration of annealing has been optimized for large crystallite size favorers larger magnetization even at weaker fields.

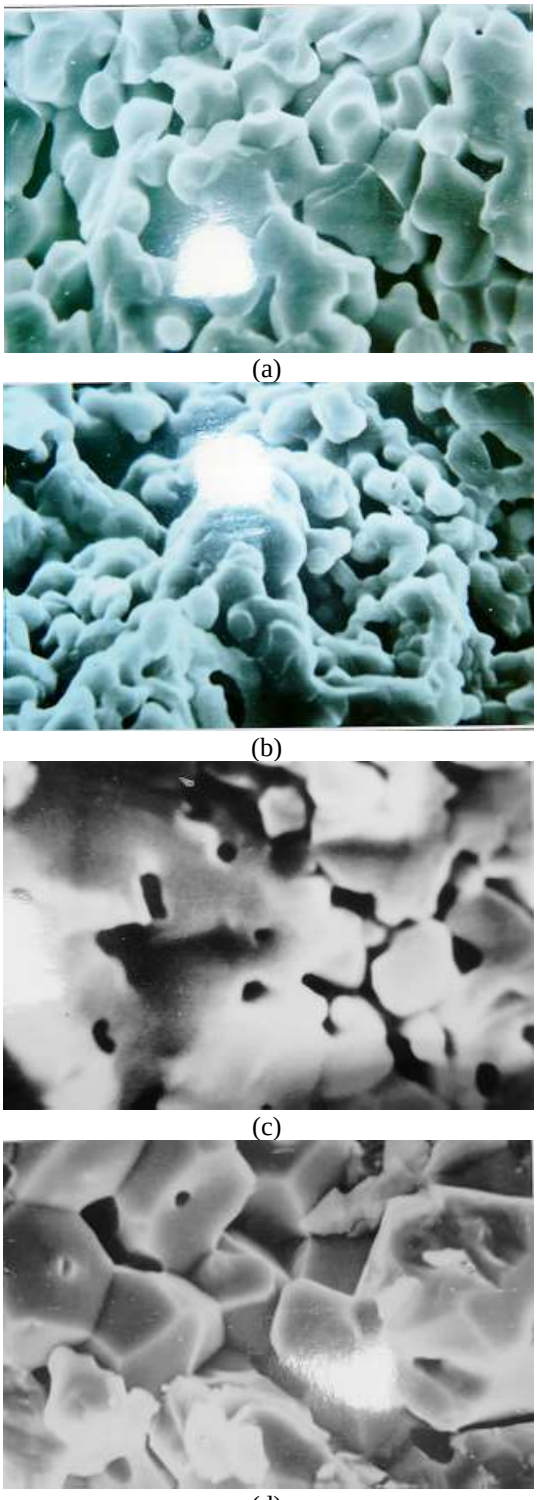

Figure.5 (a, b) SEM Photographs of CMR ($La_{1-x}Sr_xMnO_3$) annealed at 6500 C in Vacuum UHV System C. **(c, d)** SEM Photographs of CMR $la_{1-x}Sr_xMnO_3$ annealed at 13500 C 12h.

COLOSSAL MAGNOTORESISTORESISTIVITY

The metallic $La_{1-x}A_xMnO_3$ $A = Sr/Ba/Ca$ composition exhibits very high (colossal) negative magneto-resistance near T_C. The magneto-resistance is defined by $[\rho/(0) - \rho(H)/\rho(H)$ where $\rho(0)$ is the resistivity under zero field and $\rho(H)$ is the resistivity under an applied field H. In the traditional magneto-resistive systems (like granular metallic films, magnetic multilayer's etc), it varies from $2-4\%\ to\ 30-40\%$ whereas in CMR materials (especially in thin film form), it is found to be as high as ~100,000%~ (A.S.Alexandrov et al,1999).Therefore, this material proves to be a strong candidate for being used as magnetic sensors. Application of high magnetic field improves the ferromagnetic spin alignment (and T_c) which leads to strong suppression of any scattering. Increased metallicity below Tc and improvement of T_C itself give rise to CMR near T_C. Since the amount of CMR depends on the strength of the double exchange interaction along $Mn^{3+} - O^{2-} - Mn^{4+}$ bonds, it can be modified by varying the bond length and angle (θ) by suitably replacing A-site with ions of smaller radius (S.Jin et al,1994). Such replacement modifies θ, as the structure rotates and tilts to accommodate the smaller ion, which, in turn gives rise to smaller transfer integral t. The magneto-resistivity improves while the T_C degrades. Improvement of magneto-resistivity is the result of enhanced zero field resistivity. The scaling of the magneto-resistivity with the average $A-site$ radius $< A >$ and the variance σ^2 is an important observation (H.Y.Hwang et al, 1995) which helps in maneuvering the magneto-resistivity. However, such intrinsic magneto-resistivity is observed only under a high magnetic field $(1-5T)$, whereas, for any magnetic sensor application, low field $(\sim 10-100G)$ switching of magneto-resistivity is required. The physics of the intrinsic magneto resistivity lies in the interplay of charge lattice and spin degrees of freedom. Modification of any one of them modulates the amount of magneto-resistivity by a large extent. For a fixed doping level $x = 0.33$, Tc as well as the magneto-resistivity were shown to be modulated by a large extent through smaller ion substitution like Pr, Y etc at the $LA-Site$ (Jin et al., 1994). The net result of this substitution is the change in one electron bandwidth W. Effective modulation of the lattice structure is captured by the calculation of the tolerance factor t_1 which is given by $t_1 = (\Gamma_A + \Gamma_0)/\sqrt{2(\Gamma_{Mn} + \Gamma_0)}$ where Γ denotes the ionic radii of the A, Mn and O sites. It has also been shown that a phase diagram can be constructed by suitably changing the tolerance factor tl for a composition with fixed x (Figure. 4). A separate phase diagram, composed of different phase fields like canted $A-type$ antiferromagnetic insulating, ferromagnetic insulating, ferromagnetic metallic, $G-type$ antiferromagnetic insulating, paramagnetic insulating etc, can be constructed by changing x over $0.01-1.0$. Hence, it appears that a $3D$ phase space $T_C - x - t_I$ can be constructed for this class of materials. The influence of tolerance factor t_1 on the magnetoresistivity can be understood from the fact that the deviation of tl from 1.0 leads to bending of the $Mn-O-Mn$ bond. This, in turn, leads to a modulation of the transfer integral't'. The zero field resistivity, as a result of such modulation, becomes high whereas the drop in resistivity under a magnetic field is governed by enhanced ferromagnetism (and hence suppression of spin scattering) as well as modulation of the structure itself. Together they give rise to very high magnetoresistivity. Therefore, it appears that the substitution of $La-site$ by smaller ions (while the charge

carrier concentration is kept constant at $x = 0.33$) leads to high chemical pressure which, in turn, helps in evolving an entire phase diagram as well as improving the magnetoresistivity.

However, it has also been observed that even though the magnetoresistivity is improved, the T_C is degraded as a result of drop in t and W. In order to achieve optimum magnetoresistivity near room temperature, one should, therefore, optimize the structure as well as carrier concentration x, i.e. W. By creating defects through heavy ion irradiation improvement of the magneto resistivity can be achieved (Van Slyke et al., 1996). Of course, while the magnetoresistivity is found to have improved, T_C is found to have gone down. And beyond a certain radiation dosage $> 10^{15} ion/cm^2$, large scale damage of the sample could be observed. The amount of magnetoresistivity is found to have close correlation with the magnetization M/MS, where Ms is the saturation magnetization (Urushibara et al 1996). The resistivity and the magnetoresistivity are found to scale as $\sim(M/M_S)^2$ where M/M_S is given by Langevin function valid for a ferromagnetic material

$$M/M_S = B_1\left[\frac{m+b}{t}\right]:\ m = M/M_s\,; b = {}^{B}/_{\lambda M_S}\,; t = T/T_C \quad (15)$$

Where b is the exchange field, λ is the exchange coupling, B_J is the Brillouin function which is given by

$$B_J(y) = [(2J + 1/2J]\coth\left\{\frac{(2J+1)Y}{2J}\right\} - (1/2J\text{conth}(\frac{y}{2J}) \quad (16)$$

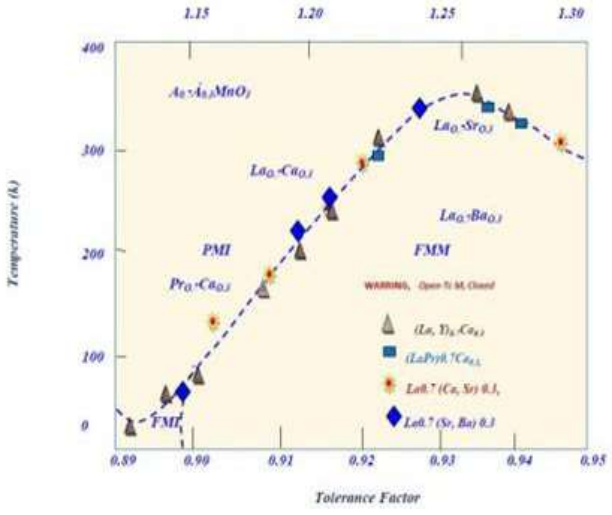

Figure.6 Phase diagram of the maganites as a function of *Tolerance Factor*

Where J is the net angular momentum. The constant of proportionality between the magnetoresistivity and $(M/M_S)^2$ depends on the carrier concentration. Recently, it has been shown that the constant of proportionality (or the scaling factor) C is equal to $x^{-2/3}$ where x is the no. of charge carriers per unit magnetic cell. This relation is found to be universal for different classes of materials ranging from ferromagnetic metals like $(Ni, Fe\ etc)$ to doped magnetic semiconductors (like $Ge_{1-x}Mn_x\ Te$, $Eu_{1-x}Gd_xTe$ etc) Figure5.

Of course, the behaviors of the perovskite manganites seem to be deviating from this universal relationship between $C = (\Delta\rho/\rho)\ /\ (M|M_S)^2$ and X. The basic idea behind this relationship is as follows. Suppression of the spin scattering below ferromagnetic transition temperature T_C is associated with metallic conduction in a host of different classes of materials and hence can be looked as a generic feature. So long as such relationship remains valid the spectrum of magnetic scattering can be constructed as a static potential. Using the Born approximation, one can then write down the scattering rate as $\int_0^{\pi}\sigma(\theta)(1-cos\theta)d\theta$ where θ is the scattering angle, and $\sigma(\theta)$ is the scattering cross-section. Relating $\sigma(\theta)$ to the spin-spin correlated function χ and hence to the susceptibility and using Ginzburg-Landau approximation one can write down the magneto resistivity $\Delta\rho/\rho\ as\ \Delta\rho/\rho = c(M/M_S)^2 \approx (\frac{1}{2K_F\xi_0})^2(M/M_S)^2$ where ζ_0 is the correlation length and K_F^{-1} is Fermi wave vector.

The correlation between C and carrier density highlights the fact that within the regime of metallic conduction and ferromagnetism the magneto resistivity depends on the scattering rate and hence on the scattering cross section. Since, C drops with the increase in X, it becomes clear that low carrier density lead to high Δρ / ρ and vice versa or in other words, small correlation length ζ_0 yields large C. Interestingly, although a range of different materials' properties can be fitted by this universal relationship Figure 5, the colossal magneto resistive manganites appear to be not following such pattern.

The deviation highlights the fact that in CMR materials the magneto resistivity is governed not only by the double-exchange induced ferromagnetism or spin-spin scattering but also by the coupling of charge carriers to the lattice degrees of freedom. In spite of large magneto resistivity observed in perovskite manganites, the switching field is found to be high $(\sim 1.5T)$. Whereas for device application, CMR under a low field $(\sim 10 - 100G)$ is required.

Therefore, extrinsic magnetoresistivity as a result of spin-polarized tunneling (Hwang et al., 1996) or grain/domain boundary scattering (Li et al., 1997) assumes importance. Extrinsic magnetoresistivity is found to be ~40% and temperature independent over a large temperature range from near T_c down to a low temperature (Venkatesan et al., 1998). The extent of extrinsic magnetoresistivity as opposed to intrinsic magnetoresistivity can be turned by the grain boundary structure.

This particular observation has brightened the prospect of utilizing the materials as different sensors. There are few recent observations where intrinsic tunneling magnetoresistivity between two magnetic unit cells of A_2BBO_6 type compounds is found to be quite sizable (Kobayashi, Kimura, Sawada, Terakura, & Tokura, 1998). One such compound is Sr_2MoFeO_6.

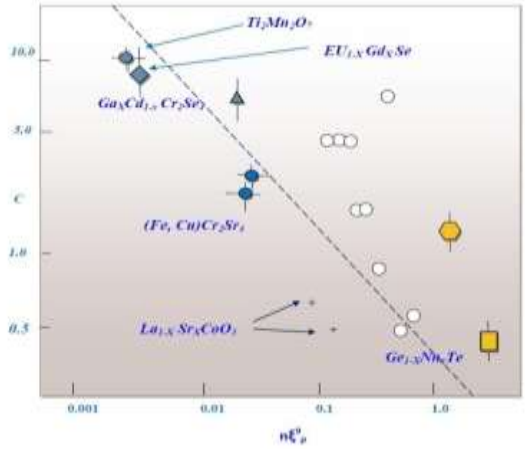

Figure.7 Universal scaling between $C(=[\Delta\rho/\rho]/(M/M_S)^2$ and the carrier density.

CONCLUSION

In this paper we have discussed physics of colossal Magneto-Resistance (CMR) materials. They are mangaintes in perovskite structures, the properties change drastically on creating lanthanum ion deficiency or replacing the by alkaline earth substituent such as Sr in $LSMO$ has thus been an example.Various Theoretical aspects such as double exchange, Jahn_Teller effect, charge and orbital ordering has been discussed, the perovskites are a 'gold mine' of transitions, the research due to new findings. And properties of $LSMO$ and related compounds are given to illustrate experimental aspects CMR effect indicates large changes in resistively occurring due to small changes in originate in the non-trivial interplay of the charge, spin, and orbital and lattice degrees of freedom in manganite materials. Theoretically at results due-to mixed-phase formation. One phase is embedded in the other. The phase as Ferromagnetic (FM) metallic. Antifenomagnetic (AF) insulating phase. This increases dc resistivity and the compressibility of the system. Thus CMR originates in inhomogenieties of phases(Mori, Chen, & Cheong, 1998). Our experiments show inhomogenieties in the pictures and large grains of each phase. Certain aspects obtainable with theoretical model calculations such as pseudo gap are left for elaboration for next paper in future

ACKNOWLEDGEMENTS

Authors acknowledge useful discussion with D. Bhattacharya of Cryogenic Division of NpL. He also wishes to acknowledge the encouragement given by Prof, A. K. Raychaudhuri, NPL, during the work.

REFERENCES

Alexandrov, A., & Bratkovsky, A. (1999). Carrier density collapse and colossal magnetoresistance in doped manganites. *Physical review letters*, *82*(1), 141.

Anderson, P. W., & Hasegawa, H. (1955). Considerations on double exchange. *Physical Review*, *100*(2), 675.

Baibich, M. N., Broto, J., Fert, A., Van Dau, F. N., Petroff, F., Etienne, P., Chazelas, J. (1988). Giant magnetoresistance of (001) Fe/(001) Cr magnetic superlattices. *Physical review letters*, *61*(21), 2472.

Bass, J., & Pratt Jr, W. (1999). Current-perpendicular (CPP) magnetoresistance in magnetic metallic multilayers. *Journal of magnetism and magnetic materials*, *200*(1), 274-289.

Bloemen, P., Van de Vorst, M., Johnson, M., Coehoorn, R., & De Jonge, W. (1994). Magnetic layer thickness dependence of the interlayer exchange coupling in (001) Co/Cu/Co. *Journal of applied physics*, *76*(10), 7081-7083.

Celotta, R., Pierce, D., & Unguris, J. (1995). SEMPA studies of exchange coupling in magnetic multilayers. *MRS Bulletin*, *20*(10), 30-33.

Chakraborty, A., Bhattacharya, D., & Maiti, H. S. (1997). Zero-field resistivity anomaly and low-field response of the canted antiferromagnetism in unsubstituted and Ba-substituted LaMnO 3+ δ within the insulating regime. *Physical Review B*, *56*(14), 8828.

De Gennes, P.-G. (1960). Effects of double exchange in magnetic crystals. *Physical Review*, *118*(1), 141.

Goodenough, J. B. (1955). Theory of the Role of Covalence in the Perovskite-Type Manganites [La, M (II)] Mn O 3. *Physical Review*, *100*(2), 564.

Honda, S., Fujimoto, T., & Nawate, M. (1996). Giant magnetoresistance of perpendicular magnetic Co/Au multilayers. *Journal of applied physics*, *80*(9), 5175-5182.

Hwang, H., Cheong, S., Ong, N., & Batlogg, a. B. (1996). Spin-polarized intergrain tunneling in La 2/3 Sr 1/3 MnO 3. *Physical review letters*, *77*(10), 2041.

Hwang, H., Cheong, S., Radaelli, P., Marezio, M., & Batlogg, B. (1995). Lattice Effects on the Magnetoresistance in Doped LaMn O 3. *Physical review letters*, *75*(5), 914.

Imada, M., Fujimori, A., & Tokura, Y. (1998). Metal-insulator transitions. *Reviews of Modern Physics*, *70*(4), 1039.

Jin, S., Tiefel, T. H., McCormack, M., Fastnacht, R., Ramesh, R., & Chen, L. (1994). Thousandfold change in resistivity in magnetoresistive La-Ca-Mn-O films. *Science*, *264*(5157), 413-415.

Jonker, G., & Van Santen, J. (1950, 1953). Magnetic compounds wtth perovskite structure III. ferromagnetic compounds of cobalt. *Physica*, *19*(1), 120-130.

Ju, H., Sohn, H.-C., & Krishnan, K. M. (1997). Evidence for O 2 p Hole-Driven Conductivity in La 1-x Sr x MnO 3 (0≤ x≤ 0.7) and La 0.7 Sr 0.3 MnO z Thin Films. *Physical review letters*, *79*(17), 3230.

Kawano, H., Kajimoto, R., Kubota, M., & Yoshizawa, H. (1996). Ferromagnetism-induced reentrant structural transition and phase diagram of the lightly doped insulator La 1-x Sr x Mn O 3 (x<~ 0.17). *Physical Review B*, *53*(22), R14709.

Kobayashi, K.-I., Kimura, T., Sawada, H., Terakura, K., & Tokura, Y. (1998). Room-temperature magnetoresistance in an oxide material with an ordered double-perovskite structure. *Nature*, *395*(6703), 677-680.

Lee, P. A., & Ramakrishnan, T. (1985). Disordered electronic systems. *Reviews of Modern Physics*, *57*(2), 287.

Li, X., Gupta, A., Xiao, G., & Gong, G. (1997). Low-field magnetoresistive properties of polycrystalline and epitaxial perovskite manganite films. *Applied physics letters*, *71*(8), 1124-1126.

Majumdar, P., & Littlewood, P. B. (1998). Dependence of magnetoresistivity on charge-carrier density in metallic ferromagnets and doped magnetic semiconductors. *Nature*, *395*(6701), 479-481.

Millis, A., Littlewood, P., & Shraiman, B. I. (1995). Double exchange alone does not explain the resistivity of La 1-x Sr x MnO 3. *Physical review letters*, *74*(25), 5144.

Mori, S., Chen, C., & Cheong, S.-W. (1998). Pairing of charge-ordered stripes in (La, Ca) MnO3. *Nature*, *392*(6675), 473-476.

Mott, N. (1961). The transition to the metallic state. *Philosophical Magazine*, *6*(62), 287-309.

Mott, N. F., & Davis, E. A. (1979). *Electronic processes in non-crystalline materials*: Oxford University Press.

Okimoto, Y., Katsufuji, T., Ishikawa, T., Arima, T., & Tokura, Y. (1997). Variation of electronic structure in La 1-x Sr x MnO 3 f as investigated by optical conductivity spectra. *Physical Review B*, *55*(7), 4206.

Palstra, T., Ramirez, A., Cheong, S., Zegarski, B., Schiffer, P., & Zaanen, J. (1997). Transport mechanisms in doped LaMnO 3: evidence for polaron formation. *Physical Review B*, *56*(9), 5104.

Rao, C., & Cheetham, A. (1997). Charge ordering in manganates. *Science*, *276*(5314), 911-912.

Speriosu, V., Nozieres, J., Gurney, B., Dieny, B., Huang, T., & Lefakis, H. (1993). Role of interfacial mixing in giant magnetoresistance. *Physical Review B*, *47*(17), 11579.

Van Slyke, S., Chen, C., & Tang, C. (1996). Organic electroluminescent devices with improved stability. *Applied physics letters*, *69*(15), 2160-2162.

Venkatesan, T., Rajeswari, M., Dong, Z.-W., Ogale, S., & Ramesh, R. (1998). Manganite-based devices: opportunities, bottlenecks and challenges. *PHILOSOPHICAL TRANSACTIONS-ROYAL SOCIETY OF LONDON SERIES A MATHEMATICAL PHYSICAL AND ENGINEERING SCIENCES*, 1661-1680.

Wollan, E., & Koehler, W. (1955). Neutron Diffraction Study of the Magnetic Properties of the Series of Perovskite-Type Compounds [(1-x) La, x Ca] Mn O 3. *Physical Review*, *100*(2), 545.

Zener, C. (1951). Interaction between the d-shells in the transition metals. II. Ferromagnetic compounds of manganese with perovskite structure. *Physical Review*, *82*(3), 403.

